Published in final edited form as:
J Neurochem. 2010 October ; 115(1): 36–46. doi:10.1111/j.1471-4159.2010.06894.x.

The G2019S Pathogenic Mutation Disrupts Sensitivity of Leucine-Rich Repeat Kinase 2 to Manganese Kinase Inhibition

Jason P. Covy[#] and **Benoit I. Giasson**[#]

[#]Department of Pharmacology, University of Pennsylvania School of Medicine, Philadelphia, Pennsylvania 19104.

Abstract

Mutations in leucine-repeat rich kinase-2 (*LRRK2*) are the most common cause of late-onset Parkinson disease. Previously, we showed that the G2019S pathogenic mutation can cause a dramatic increase (~10 fold) in kinase activity, far above other published studies. A notable experimental difference was the use of Mn-ATP as a substrate. Therefore, the effects of metal cation-ATP cofactors on LRRK2 kinase activity were investigated. It is shown, using several divalent metal cations, that only Mg^{2+} or Mn^{2+} can support LRRK2 kinase activity. However, for wild-type, I2020T and R1441C LRRK2, Mn^{2+} was significantly less effective at supporting kinase activity. In sharp contrast, both $Mn^{2+}$and Mg^{2+} were effective at supporting the activity of G2019S LRRK2. These divergent effects associated with divalent cation usage and the G2019S mutation were predominantly due to differences in catalytic rates. However, LRRK2 was shown to have much lower (~40 fold) ATP K_m for Mn-ATP compared to Mg-ATP. Consequently, sub-stoichiometric concentrations of Mn^{2+} can act to inhibit the kinase activity of wild-type, but not G2019S LRRK2 in the presence of Mg^{2+}. From these findings, a new model is proposed for a possible function of LRRK2 and the consequence of the G2019S LRRK2 pathogenic mutation.

Keywords

Kinase; LRRK2; magnesium; manganese; Parkinson disease

Introduction

Parkinson disease (PD) is the second most prevalent neurodegenerative disease in the developing world, and is believed to result from complex genetic and environmental factors. It is characterized clinically by resting tremor, bradykinesia, postural instability, and muscle rigidity (Hoehn and Yahr 1967;Simuni and Hurtig 2000). Although primarily viewed as an idiopathic disease, a number of gene defects have been established to either cause or increase the risk of PD [reviewed in (Ross and Farrer 2005;Forman et al. 2005;Henchcliffe and Beal 2008;Bonifati 2007;Biskup et al. 2008;Thomas and Beal 2007)]. More specifically, autosomal dominant missense mutations in the gene for *leucine-rich repeat kinase 2* (*LRRK2/PARK8*) are the most common known cause of PD (Zimprich et al. 2004;Paisan-Ruiz et al. 2004;Giasson and Van Deerlin, 2008). At least 5 LRRK2 missense mutations are considered definitely pathogenic, but many other amino acid substitutions within this protein have been linked to PD (see Fig. 1A) (Zimprich et al. 2004;Paisan-Ruiz et al. 2004;Mata et al. 2006;Taylor et al. 2006;Biskup and West 2008;Giasson and Van Deerlin, 2008). The

Address correspondence to: Dr. Benoit I. Giasson, Department of Pharmacology, University of Pennsylvania School of Medicine, 125 John Morgan Building, 3620 Hamilton Walk, Philadelphia, PA 19104-6084. Tel: 215-573-6012; Fax: 215-573-2236; giassonb@mail.med.upenn.edu.

most prevalent mutation, G2019S, is reportedly responsible for 0.6–1.6 % of sporadic PD (Deng et al. 2005;Gilks et al. 2005;Kachergus et al. 2005) and 2–8 % of familial PD cases (Paisan-Ruiz et al. 2005;Deng et al. 2005;Di Fonzo et al. 2005;Kachergus et al. 2005;Hernandez et al. 2005;Nichols et al. 2005). In certain ethnicities, such as North African Arabs and Ashkenazi Jews, the G2019S mutation is even a greater factor contributing to PD (22–41% of individuals with disease) (Lesage et al. 2005;Ozelius et al. 2006;Lesage et al. 2006).

LRRK2 is a widely-expressed 2527 amino acid protein with several discrete domains (Fig. 1A) (Zimprich et al. 2004;West et al. 2007;Paisan-Ruiz et al. 2004). Containing a Ras-of-complex (ROC)/GTPase domain followed by a C-terminal of RAS (COR) domain, it is a member of the ROCO protein family (see Fig. 1A). The LRRK2 kinase domain displays highest sequence homology to the mixed-linage kinase subfamily of mitogen-activated protein kinase kinase kinases, so named due to kinase sub-domain structures resembling both protein Y- and S/T-kinases (West et al. 2005;West et al. 2007;Manning et al. 2002). To date it has been shown that LRRK2 can function as a S/T-kinase that can undergo autophosphorylation (Smith et al. 2006;West et al. 2007;West et al. 2005;Covy and Giasson 2009;Anand et al. 2009;Luzon-Toro et al. 2007;Greggio et al. 2008;Jaleel et al. 2007); although its ability to function as a Y-kinase has not been rigorously investigated. Some modeling studies have suggested that LRRK2 may be a dual specificity kinase, phosphorylating both S/T and Y residues (Manning et al. 2002;West et al. 2007), but so far it has been shown to function predominantly as a S/T-kinase (Anand et al. 2009;West et al. 2007) and only weak activity towards the Y-kinase substrate poly(E)tyrosine was reported (West et al. 2005). Furthermore, the biological functions and regulation of LRRK2, and the effects of disease-causing mutations therein are still ill-defined (Biskup and West, 2008;Greggio and Cookson 2009;Webber and West, 2009). For example, the R1441C mutation was demonstrated to increase kinase activity in some studies (West et al. 2005;West et al. 2007), but others have reported no significant change (Greggio et al. 2006;Jaleel et al. 2007;Gloeckner et al. 2009;Anand et al. 2009). The I2020T mutation was documented to either modestly increase (West et al. 2007;Gloeckner et al. 2006;Gloeckner et al. 2009), show no change (Anand et al. 2009) or decrease kinase activity (Jaleel et al. 2007). Most studies of the G2019S mutation demonstrated increased kinase activity, although modest (2–3 fold) (Greggio et al. 2006;West et al. 2005;West et al. 2007;Jaleel et al. 2007;Gloeckner et al. 2009;Anand et al. 2009). Recently, we have shown that in one experimental paradigm, the G2019S LRRK2 mutant can demonstrate 10-fold greater kinase activity than wild-type (WT) LRRK2 (Covy and Giasson 2009). One notable difference is that we used Mn^{2+} as an ATP cofactor, while most other published studies have used Mg^{2+}. Therefore, in this study we assessed the relative kinetic effects of Mg^{2+} versus Mn^{2+} on the catalytic properties of WT LRRK2 and some disease-causing mutants thereof.

Materials and Methods

Materials

Goat anti-glutathione-S-transferase (GST) polyclonal antibody was purchased from Amersham Biosciences (Piscataway, NJ). The shuttling vector pCR8/GW/TOPO and the mammalian expression GST-tagged vector pDEST27 were purchased from Invitrogen (Carlsbad, CA). LRRKtide (RLGRDKYKTLRQIRQ), LRRKtide-TA (RLGRDKYKALRQIRQ) that is deficient in S/T residues, LRRKtide-YF (RLGRDKFKTLRQIRQ) that is deficient in Y residues, and Nictide (RLGWWRFYTLRRARQGNTKQR) were synthesized and purified on reverse phase HPLC by GenScript USA Inc. (Piscataway, NJ). The synthetic peptides MBP fragment 104–118 (GKGRGLSLSRFSWGA), Kemptide (LRRASLG), and caesin kinase 2 substrate (RRRADDSD) were purchased from Sigma-Aldrich (St. Louis, MO). The synthetic peptides

MBP fragment 4–14 (KRPSQRSKYL), MBP fragment 94–102 (APRTPGGRR), MARCKS PSD-derived peptide (KKRFSFKKSFKL), and PKC_{δ} peptide substrate (RFAVRDMRQTVAVGVIKAVDKK) were obtained from Calbiochem/EMD Biosciences (Gibbstown, NJ). Kinase inhibitors JAK3 VI, K252-A, PKR, ROCK-IV, and staurosporine were purchased from Calbiochem/EMD Biosciences, and sunitinib was purchased from Sigma-Aldrich.

Cell Culture

Human embryonic kidney 293T cells were cultured in Dulbecco's modified medium with high glucose (4.5gm/L) supplemented with 10 % fetal bovine serum, 100U/ml penicillin, 100U/ml streptomycin, and 2 mM L-glutamine.

LRRK2 Expression Constructs

The full-length human LRRK2 cDNA was amplified by PCR using Taq polymerase AccuPrime SuperMix (Invitrogen) and cloned by topoisomerase reaction into the shuttling vector pCR8/GW/TOPO. To generate the cDNAs encoding the G2019S or I2020T mutations, the LRRK2 cDNA fragment spanning the AvrII and NcoI restriction sites in LRRK2 was amplified by PCR and cloned by topoisomerase reaction into the vector pCR4-TOPO (Invitrogen). To generate the cDNA encoding the R1441C mutation, the LRRK2 cDNA fragment spanning the NdeI and SpeI restriction sites in LRRK2 was amplified by PCR and cloned by topoisomerase reaction into the vector pCR4-TOPO (Invitrogen). The mutations corresponding to the R1441C, G2019S or I2020T amino acid substitutions, respectively, were generated using the QuickChange® Site Directed Mutagenesis Kit (Stratagene, La Jolla, CA). The AvrII/NcoI DNA fragments containing either the G2019S or I2020T mutants or the NdeI/SpeI DNA fragments containing the R1441C mutation were reintroduced into full-length LRRK2 by subcloning with these restriction enzymes. The sequence of the plasmids was verified by DNA sequencing using primers that span the whole cDNA as a service offered by the DNA Sequencing Facility of the University of Pennsylvania. WT and mutant full-length LRRK2 cDNAs were introduced into the pDEST27 vector by recombinase reaction using LR Clonase II enzyme (Invitrogen) to generate a plasmid expressing N-terminal GST-tagged protein.

Western Blotting Analysis

Proteins were resolved on SDS-polyacrylamide gels by SDS-PAGE and electrophoretically transferred onto nitrocellulose membranes (Bio-Rad Laboratories, Hercules, Ca) in buffer containing 190 mM glycine, 25 mM Tris-base and 10% methanol. Membranes were blocked with a 5% powdered skimmed milk solution dissolved in Tris buffered saline (50 mM Tris, pH 7.6, 150 mM NaCl), incubated with anti-GST antibody followed with an anti-goat antibody conjugated to horse radish peroxidase, developed with Western Lightning Chemiluminescence Reagents (PerkinElmer Life Sciences (Boston, MA) and exposed onto X-Omat Blue XB-1 films (Kodak, Rochester, NY).

In-vitro LRRK2 Kinase Assays

293T cells were transiently transfected with pDEST27/LRRK2 expression plasmid using calcium phosphate precipitation method buffered with N, N-bis(2-hydroxyethyl)-2-amino-ethanesulfonic acid (BES) (Chen and Okayama 1997). 48–72 hours after transfection, cells were washed and harvested with PBS, and resuspended in lysis buffer (25 mM Tris pH 7.4, 150 mM NaCl, 5 mM EDTA, 10 mM beta-glycerol phosphate, 1 mM $NaVO_4$, 1 % Triton X-100, 0.5% glycerol with protease inhibitor cocktail) at 4°C. Cell debris were removed by sedimentation at 13,000×g for 15 minutes, and supernatants were precleared by incubation with sepharose beads that were removed by sedimentation. Supernatants were incubated

with glutathione-sepharose beads (GE Healthcare) for 3 hours at 4°C. Beads were extensively washed with lysis buffer (5 times) and wash buffer (25 mM Hepes, pH. 7.4, 1mM DTT, 10 mM β-glycerophosphate)(5 times) and eluted with wash buffer with 20mM glutathione. The kinase reactions were conducted at 25ºC by incubating purified GST-LRRK2 in 25 μL of kinase buffer (25 mM Hepes, pH. 7.4, 10 mM β-glycerophosphate), with the added specified divalent cation, and varying [γ-^{32}P]ATP (4 Ci/mmoles) (1 μM to 800 μM) and LRRKtide peptide (1 μM to 1200 μM) concentrations as specified for each experiment. All reactions were conducted for 60 minutes at 25°C, except for the time course experiments that were conducted for the indicated times. Reactions were applied to individual 2.5 cm-diameter disks of P-81 phosphocellulose filter paper (Schleicher & Schuell) that were immediately immersed in 75 mM phosphoric acid. After extensive wash with 75 mM phosphoric acid, P-81 filters were rinsed with acetone and allowed to air dry. Filters were immersed in Cytoscint liquid scintillation cocktail (Fisher Scientific) and ^{32}P radioactivity on each filter was measured by liquid scintillation using an LS6500 counter (Beckman Coulter). A unit of LRRK2 activity was defined as the amount of enzyme that catalyzed the incorporation of 1 pmol of ^{32}P into LRRKtide. K_m and V_{max} parameters were calculated using Graph-Pad Prism v5.01.

For autophosphorylation of LRRK2, reactions were stopped with the addition of sodium dodecyl sulfate (SDS) sample buffer and heating to 100°C for 5 min. Samples were resolved onto 6% SDS-polyacrylamide gels, dehydrated in a 50% Methanol, 10% glycerol, 10% acetic acid solution, dried and exposed to a PhosphorImager plate (Molecular Dynamics, Piscataway, NJ), and visualized using ImageQuant software (Molecular Dynamics, Inc., Sunnyvale, CA).

Results

We recently generated a novel system to purify substantial amounts of active recombinant full-length LRRK2 expressed in 293T mammalian cells (Covy and Giasson 2009). In this system, LRRK2 is expressed as an N-terminal tagged GST protein that is purified using glutathione-sepharose beads as described in “Materials and Methods”. The kinase activity of this enzyme was previously characterized for specificity using a kinase dead version as well as kinase inhibitors in the presence of Mn^{2+}(Covy and Giasson 2009). The specificity of this activity was further confirmed using a series of previously published and characterized LRRK2 kinase inhibitors (Anand et. al., 2009; Reichling and Riddle, 2009; Nichols et al. 2009) in the presence of Mg^{2+} (Supplemental Fig. 1). For the studies described here, WT and 3 pathogenic mutants of LRRK2 (R1441C, G2019S, and I2020T) were purified to equivalent levels (Fig. 1B). The kinase reactions in the present studies were conducted using the synthetic peptide LRRKtide that spans residue T558 of moesin, which was previously identified as a robust in vitro substrate for LRRK2 (Jaleel et al. 2007;Covy and Giasson 2009;Anand et al. 2009).

Protein kinases require the formation of an ATP-divalent metal complex for the phosphoryl transfer of the γ-phosphate of ATP to a protein substrate (Knowles 1980). Typically, Mg^{2+} serves as the essential metal ion for catalysis, however Mn^{2+} and other divalent cations may support nucleotide binding and subsequent use as a cofactor for phosphoryl transfer (Elberg et al. 1995;Koland and Cerione 1990;Courtneidge 1985;Sun and Budde 1997;Toru-Delbauffe et al. 1986). Several divalent metal cations were tested to assess their ability to act as an ATP cofactor for WT and pathogenic variants of LRRK2. This analysis was conducted for pathological mutations within the active site (G2019S and I2020T) as well as a pathological mutation distinct from this site (R1441C). Of the divalent metal cations assessed, Mg^{2+} demonstrated the greatest ability to support LRRK2 kinase activity under the reaction conditions used here (200 μM ATP, 400 μM LRRKtide) (Fig. 1C). Mn^{2+} also

demonstrated a modest ability to promote LRRK2 kinase activity of WT, R1441C and I2020T LRRK2, however this property was greatly enhanced for the G2019S LRRK2 mutant. The other divalent cations tested were not able to support LRRK2 kinase activity.

It is well known that many Y-kinases prefer Mn^{2+} as an ATP cofactor (Elberg et al. 1995;Koland and Cerione 1990;Courtneidge 1985;Sun and Budde 1997;Hunter and Cooper 1985), and for some dual specificity kinases, the presence of Mn^{2+} versus Mg^{2+} can cause a switch in preferential activity from a protein S/T-kinase to a protein Y-kinase (Yuan et al. 1993;Huang et al. 1994) . Therefore, it is possible that Mn^{2+} may support the activity of LRRK2 as a Y-kinase since LRRKtide (RLGRDKYKTLRQIRQ) contains both a T and a Y residue. To further investigate the type of kinase activities associated with the use of Mg^{2+} or Mn^{2+}, kinase reactions for WT, R1441C, G2019S, and I2020T LRRK2 were performed in the presence of 5 mM Mg^{2+} or Mn^{2+} and LRRKtide, LRRKtide deficient in S/T residues (LRRKtide-TA; RLGRDKYKALRQIRQ) or LRRKtide that is deficient in Y residues (LRRKtide-YF; RLGRDKFKTLRQIRQ). Results showed that only LRRKtide with a T residue served as a substrate for LRRK2 in the presence of Mg^{2+} or Mn^{2+} (Fig. 1D). To further confirm that the persistence of kinetic activity of the G2019S mutant in the presence of Mn^{2+} is not a result of altered substrate specificity, a number of other characterized synthetic peptides with known kinase recognition motifs, including the engineered LRRK2 substrate Nictide (Nichols et al., 2009), were analyzed in the presence of Mg^{2+} or Mn^{2+}, and no differences in substrate recognition were observed (Supplemental Fig. 2).

Time course analysis of the kinase activity for WT, R1441C, G2019S, and I2020T LRRK2 in the presence of Mg^{2+} or Mn^{2+} was performed to determine the consistent progress of the phosphoryl transfer over time. Results showed that the kinase reaction was linear over the course of two hours, allowing extrapolation of initial velocity and confirming that differences in kinetic activity were not due to changes in kinase stability (Fig. 1E). In addition, similar to our initial screen of divalent cations, WT, R1441C, G2019S, and I2020T LRRK2 kinase activity was much greater in the presence of Mg^{2+} compared to Mn^{2+} for all enzymes except the G2019S mutant.

To further investigate the effects of Mg^{2+} and Mn^{2+} on LRRK2 kinase activity, the ability and extent of each ion to support kinase activity was assessed by varying their concentrations. For all variants of LRRK2 assayed against LRRKtide, increasing the concentration of Mg^{2+} resulted in increased kinase activity with maximum activity at 5 mM. Mn^{2+} also supported the kinase activity of LRRK2, but maximal activity was observed at ~ 0.5 mM and all variants demonstrated a similar relative decrease in activity at higher concentrations with ~ 2-fold lower activity at 5 mM Mn^{2+} compared to 0.5 mM Mn^{2+} (Fig. 2). R1441C and I2020T mutants demonstrated Mn^{2+} concentration activity profiles that were similar to WT LRRK2, but G2019S LRRK2 revealed dramatically greater activity than the other LRRK2 variants in the presence of Mn^{2+} and this was especially striking in the presence of Mn^{2+} below or near sub-stoichiometric concentrations of ATP. These effects were replicated using the synthetic substrate Nictide (Supplemental Fig. 3). Again, Mn^{2+} is capable of driving kinase activity, although not to the extent of Mg^{2+} for WT, R1441C, and I2020T LRRK2. For G2019S LRRK2, Mn^{2+} demonstrated the ability to drive much greater kinase activity than for the other LRRK2 variants, and in fact, G2019S LRRK2 showed greater kinase activity in the presence of Mn^{2+} compared to Mg^{2+} (Supplemental Fig. 3C). Although the effects of Mg^{2+} and Mn^{2+} on WT, R1441C, G2019S and I2020T LRRK2 kinase activity using either LRRKtide or Nictide are consistent, there are some relative differences and more detailed kinetic studies of the difference between LRRKtide and Nictide are under investigation.

Similar results for divalent cation preference were observed for autophosphorylation of LRRK2. Increasing concentrations of Mg^{2+} drove robust autophosphorylation of both WT and G2019S LRRK2, and these levels were greatly reduced in the presence of Mn^{2+} for WT, but not G2019S (Fig. 3A). Interestingly, 0.1 mM Mn^{2+} induced higher autophosphorylation activity in both WT and G2019S LRRK2 compared to Mg^{2}. This selectivity may reflect higher affinity for ATP-Mn (see below), but direct affects of divalent cations on LRRK2 autophosphorylation cannot be excluded and this will require further detailed analyses. Nevertheless, consistent with LRRKtide, WT LRRK2 exhibited lower autophosphorylation activity in 5 mM Mn^{2+} versus 5 mM Mg^{2+}, while G2019S LRRK2 displayed similar autophosphorylation in the presence of either 5 mM Mn^{2+}or Mg^{2+} (Fig. 3B).

To investigate the nature of the differences in the kinetics properties affected by Mg^{2+} versus Mn^{2+} and the provocative effects of the G2019S LRRK2 pathogenic mutation, the Michaelis-Menton parameters were determined for WT, R1441C, I2020T, and G2019S LRRK2 using LRRKtide as a substrate . To ensure that the ATP-cation complex was at saturating levels, 5 mM Mg^{2+} or Mn^{2+} was used to remain at a concentration several fold above the highest concentration of ATP. Furthermore, results showed at this concentration of Mg^{2+}, maximal LRRK2 activity is obtained. Kinetic analyses for the K_m of LRRKtide, while keeping the ATP concentration constant at 200 μM, revealed values consistent with previous reports utilizing Mg^{2+} and N-terminally truncated versions ($LRRK2_{1326–2527}$ or $LRRK2_{970–2527}$) of LRRK2 (Nichols et al. 2009;Jaleel et al. 2007;Anand et al. 2009). The affinity for LRRKtide was not dramatically affected by the use of Mg^{2+} and $Mn^{2+,}$ or by mutations in LRRK2; although some subtle changes were observed (Fig. 4 and Table 1). The apparent V_{max}'s measured under these conditions revealed that WT, I2020T and R1441C LRRK2 had much greater relative catalytic rates (~10 fold) in the present of Mg^{2+} versus Mn^{2+}. In regards to each respective cation, the R1441C and I2020T mutants resulted in only small changes in catalytic rate compared to WT, while the apparent V_{max} for G2019S in the presence of Mg^{2+} was ~2.5-fold greater than WT LRRK2. However the most dramatic effect was the relative maintenance of catalytic activity of G2019S LRRK2 in the presence of Mn^{2+} relative to Mg^{2+}. This effect was unique to the G2019S mutation. In fact, for G2019S LRRK2, the V_{max} in the presence of Mn^{2+} compared to Mg^{2+} was only ~ 1.5 fold lower, in contrast to the ~9 fold lower activity for WT, R1441C, and I2020T LRRK2.

The determination of the apparent K_m of ATP while keeping LRRKtide constant at 400 μM revealed that WT LRRK2 and LRRK2 mutants have a significantly lower ATP K_m in the presence of Mn^{2+} compared to Mg^{2+} (Fig. 5 and Table 2). This suggests a greater affinity for Mn-ATP than Mg-ATP. ATP K_m for WT and R1441C had similar properties, while I2020T LRRK2 had a relative lower ATP K_m in the presence of either Mg^{2+} or Mn^{2+}, respectively. Conversely, G2019S LRRK2 demonstrated relatively higher ATP K_m in the presence of either Mg^{2+} or Mn^{2+}, respectively, compared to WT LRRK2. Again, the analyses to assess V_{max} values showed that WT LRRK2 demonstrated a greater catalytic rate in the presence Mg^{2+} versus Mn^{2+}, however, the most striking finding was the much higher V_{max} for G2019S LRRK2 in the presence of Mn^{2+} compared to WT and other mutants of LRRK2.

Since under physiological conditions, Mn^{2+} exists at sub-stoichiometric concentrations relative to Mg^{2+}, we compared the relative effects of varying sub-stoichiometric concentrations of Mn^{2+} in the presence of a fixed concentration of Mg^{2+}. For these experiments, Mg^{2+} was maintained at 5 mM while the concentration of Mn^{2+} was varied between 0–5 mM. Increasing the concentration of Mn^{2+} resulted in reduced kinase activity for WT, R1441C and I2020T LRRK2 (Fig. 6A,B,D), consistent with a greater affinity for Mn-ATP versus Mg-ATP paired with a reduction in catalytic activity when utilizing Mn-ATP. In sharp contrast, increases in the concentration of Mn^{2+} between 0.1–1 mM increased

the kinase activity of G2019S LRRK2, while only modestly reducing kinase activity at 5 mM Mn^{2+} (Fig. 6C). Given that G2019S LRRK2 levels of kinase activity in the presence of Mn^{2+} reaches a maximum at ~1 mM and that this activity is similar to G2019S LRRK2 in the presence of 5 mM Mg^{2+} (Fig. 2C), but that 5 mM Mg^{2+} in the presence of 0.1 or 0.5 mM Mn^{2+} results in higher activity, it is possible that Mn^{2+} may additionally modulate kinase activity by acting at a second site. Overall, these results are consistent with those reported recently (Lovitt et al., 2010) and show that at millimolar concentrations of Mg^{2+}, micromolar concentrations of Mn^{2+} decrease the levels of LRRK2 kinase activity, while the G2019S mutation causes a loss of this negative regulation, if not reversing the effect and increasing activity.

Discussion

In stark contrast to several other published findings (Greggio et al. 2006;West et al. 2005;West et al. 2007;Jaleel et al. 2007;Gloeckner et al. 2009;Anand et al. 2009), we recently demonstrated that the G2019S mutation in LRRK2 could result in a much greater kinase activity relative to WT LRRK2 (Covy and Giasson 2009). A notable difference in our study was the use of Mn^{2+} as an ATP cofactor compared to the use of Mg^{2+} in other studies. This led us to investigate the ability of divalent metal cations to support the kinase activity of WT and several pathogenic mutants of LRRK2. It was shown that only Mg^{2+} or Mn^{2+} could be used as ATP cofactors to support the kinase activity of LRRK2, and for WT, I2020T and R1441C LRRK2, Mg^{2+} was a much better cofactor at promoting kinase activity. Remarkably, both $Mn^{2+}$and Mg^{2+} were effective at promoting the activity of G2019S LRRK2. Using LRRKtide peptides deficient in either T or Y resides, it was shown that WT and mutants of LRRK2 appear to be exclusively S/T-protein kinases, and Mn^{2+} does not change this specificity. Furthermore, no changes in specificity were observed for a number of known generic kinase substrates for WT or G2019S LRRK2 when utilizing Mn^{2+} or Mg^{2+}. Interestingly, LRRK2 demonstrated greater activity towards the LRRKtide-YF peptide compared to LRRKtide, however, this is consistent with a previous study mapping the preferred consensus motif of LRRK2 substrates where it has been shown that for the P-2 position, an F is favored over a Y residue (Nichols et al. 2009).

Assessment of Michaelis-Menton parameters showed that the use of Mn^{2+} versus Mg^{2+} did not dramatically affect LRRKtide K_m. Consistent with previous reports using N-terminally truncated versions of LRRK2 (Reichling and Riddle 2009;Anand et al. 2009), ATP K_m for G2019S LRRK2 was higher compared to WT LRRK2, while that of I2020T LRRK2 was lower in the presence of Mg^{2+}. WT and all mutants of LRRK2 demonstrated significantly lower ATP K_m for Mn-ATP compared to Mg-ATP, and similar findings have been attributed predominantly to a high affinity for Mn-ATP (Lovitt et al. 2010). WT, R1441C and I2020T LRRK2 showed slower catalytic rates in the presence of Mn^{2+} compared to Mg^{2+}. A dramatically higher V_{max} for G2019S in the presence of Mn^{2+} compared to WT LRRK2 is the predominant reason for the ~10 fold greater level of kinase activity for G2019S LRRK2 versus WT LRRK2 that we previously reported (Covy and Giasson 2009). Consistent with these data, similar findings were observed in a recent study using a truncated version ($LRRK2_{970–2527}$) of LRRK2 expressed and purified from baculovirus-infected insect cells (Lovitt et al. 2010). However, the differences in ATP K_m for the different LRRK2 variants also indicate that relative kinase activity can be affected depending on the concentration of ATP used in the reactions, especially around or below the K_m. In the presence of Mg^{2+}, the relative difference in kinase activity for G2019S versus WT LRRK2 is usually ~2 fold greater as reflected by the V_{max} values.

The molecular basis for the differences in catalytic rates between using Mg^{2+} versus Mn^{2+} are not clear and will require comprehensive structural analysis. However, it is possible that

both metal cations may coordinate the placement and interactions of divalent cation-ATP in the binding site differently, as such affecting the rate of the phosphoryl-transfer step. Alternatively, reduced rate of cation-ADP release, which can be a rate limiting step in protein kinase phosphorylation, may be the major property affected by Mn^{2+}. Indeed, Lovitt and colleagues have shown that LRRK2 displays a higher affinity for ADP in the presence of Mn^{2+} compared to Mg^{2+} (Lovitt et al., 2010).

The dramatic alterations in the catalytic properties of LRRK2 in the presence Mn^{2+} caused by the G2019S mutation and the greater activity of this mutant is conceptually consistent with the role of this residue in the active site. G2019 is part of the highly conserved DFG motif in subdomain VII of the kinase domain (Kannan and Neuwald 2005;Hanks et al. 1988), and the D residue in this motif is involved in Mg^{2+} binding and proper coordination of Mg-ATP in the active site (Levinson et al. 2006;Karlsson et al. 1993;Taylor and Radzio-Andzelm 1994;De Bondt et al. 1993). The relative higher ATP K_m, especially in the presence of Mn^{2+}, compared to WT LRRK2, suggests that a more rapid exchange of Mn-ATP/ADP at the active site may be partially responsible for the increased catalytic rate of G2019S LRRK2 in the presence of Mn^{2+}. The DFG motif is located at the N-terminal hinge region of the activation loop that switches from an open and extended conformation in the active state to a more closed conformation in the inactive state (Kannan and Neuwald 2005;Taylor and Radzio-Andzelm 1994;De Bondt et al. 1993), and this G residue is thought to play an important role in inducing proper orientation of the D residue (Kornev et al. 2006). After inactivation, the G residue usually performs an extreme twist, thereby facilitating this D residue to turn away from the catalytic site. The lack of a side chain is thought to allow the G residue to make this turn with little steric hindrance. The G2019S mutation may disrupt the ability of this movement, and could keep the D residue positioned in the active site for longer activation periods that may also contribute to a greater catalytic rate. Nevertheless, comprehensive structural analyses will be required to better understand the molecular affects of the G2019S mutation.

The I2020T mutation, which changes the first residue following the DFG-motif, did not have a dramatic affect on the kinase kinetic properties as did the G2019S mutation. Nevertheless, consistent with other studies (Reichling and Riddle 2009) the I2020T mutation demonstrated significantly reduced ATP K_m for ATP.

Studies of the effects of Mg^{2+} on the observed LRRK2 kinase activity indicate that increasing the concentration of Mg^{2+} beyond what is needed to saturate total ATP results in further activation of LRRK2. Lovitt and colleagues recently reported comparable data using a truncated version of LRRK2 ($LRRK2_{970–2527}$) (Lovitt et al. 2010). Such an effect has been observed for several other kinases and in some cases has been attributed to a second Mg^{2+} binding site (Sun and Budde 1997;Saylor et al. 1998). Increasing the concentration of Mg^{2+} or Mn^{2+} up to 0.5 mM in the presence of 200 μM ATP increases LRRK2 kinase activity, but that is likely predominantly due to increasing the effective concentration of the cation-ATP complex. The data from Mg^{2+}/ Mn^{2+} competition assays with G2019S LRRK2 also suggest that between 0.1–0.5 mM, Mn^{2+} may also promote the kinase activity of LRRK2 independently of increasing Mn-ATP concentration. In contrast to Mg^{2+}, increasing the concentration of Mn^{2+} beyond 2 mM had an inhibitory affect on LRRK2 kinase activity, and a similar inhibitory effect observed by Lovitt and colleagues was attributed to decreased catalytic turnover (Lovitt et al. 2010). In our studies, all LRRK2 variants demonstrated similar relative decreases in activity with increasing Mn^{2+} beyond 2 mM, although for G2019S LRRK2, kinase activity remained relatively high at all concentrations of Mn^{2+} compared to WT and other mutants of LRRK2.

These enzymatic kinetic properties of LRRK2 may be more than just interesting in vitro experiments and may reflect important characteristics of this enzyme that were designed for biological functionality. Manganese is an essential metal that is widely used in certain manufacturing industries. Environmental or occupational exposure to high manganese levels can cause neurotoxicity with the development of a form of parkinsonism known as manganism (Perl and Olanow 2007;Dobson et al. 2004). Mn^{2+} is required for many enzymes and its levels in tissue are usually stable, but it can accumulate in certain brain regions, including the basal ganglia, following elevated exposure (Perl and Olanow 2007;Dobson et al. 2004). The homeostatic level of free Mn^{2+} in cells is maintained by various transporters and by binding to various proteins (Dobson et al. 2004;Au et al. 2008). It is widely believed that in vivo, Mg^{2+} is the major ATP cofactor involved in kinase reactions because of its higher abundance compared to any other divalent metal cation. However, given the much greater affinity of LRRK2 for Mn-ATP compared to Mg-ATP (~40 fold lower K_m), and our studies of the effects of sub-stoichiometric concentration of Mn^{2+} on Mg^{2+}-mediated LRRK2 kinase activity, it is possible that Mn^{2+} may act as a potent inhibitor of LRRK2 kinase activity in vivo. As seen here, in the presence of Mg^{2+}, co-incubation with 100 fold lower concentrations of Mn^{2+} cause a significant reduction in the kinase activity of WT LRRK2; however this effect does not apply to the G2019S mutant, where no activity is lost. Therefore, we hypothesize that LRRK2 may act as a sensor for increased cytoplasmic Mn^{2+} levels, which results in decreased kinase activity that would modulate downstream counteractive measures. As a consequence of its alterations in kinetic properties, it is predicted that the G2019S mutant would remain largely active at physiologically elevated Mn^{2+} levels and therefore this putative signaling pathway should be compromised. Though it can be difficult to directly demonstrate altered changes in enzyme activity in vivo as a consequence of alterations in specific ion levels, some in vivo studies have shown that elevated Mn^{2+} levels can decrease the activity of some kinases (Puli et al., 2006). Direct in vivo studies of the proposed model of the effects of Mn^{2+} on WT and G2019S LRRK2 kinase activity are complicated by the many conflicting studies of the effects of LRRK2 on signal transduction pathways and the lack of robust specific in vivo markers of LRRK2 activity (Biskup and West, 2008;Greggio and Cookson 2009; Webber and West, 2009), but in vivo studies of Mn^{2+} affects on LRRK2 kinase activity are currently under investigation. Nevertheless, the studies described here provide important insights into the kinetic properties of the kinase activity of LRRK2 and pathogenic mutants as affected by divalent metal cations.

Supplementary Material

Refer to Web version on PubMed Central for supplementary material.

The abbreviations used are

COR	C-terminal of RAS
GST	glutathione-S-transferase
LRRK2	leucine-repeat rich kinase-2
PD	Parkinson disease
ROC	Ras-of-complex
WT	wild-type

Acknowledgments

This work was funded by grants from the National Institute of Neurological Disorders and Stroke (NS053488), the University of Pennsylvania Institute on Aging and The Ellison Medical Foundation.

References

Anand VS, Reichling LJ, Lipinski K, et al. Investigation of leucine-rich repeat kinase 2 : enzymological properties and novel assays. FEBS J. 2009; 276:466–478. [PubMed: 19076219]

Au C, Benedetto A, Aschner M. Manganese transport in eukaryotes: the role of DMT1. Neurotoxicology. 2008; 29:569–576. [PubMed: 18565586]

Biskup S, Gerlach M, Kupsch A, Reichmann H, Riederer P, Vieregge P, Wullner U, Gasser T. Genes associated with Parkinson syndrome. J. Neurol. 2008; 255 Suppl. 5:8–17. [PubMed: 18787878]

Biskup S, West AB. Zeroing in on LRRK2-linked pathogenic mechanisms in Parkinson's disease. Biochim Biophys Acta. 2008; 1778:1881–1896. [PubMed: 17880914]

Bonifati V. Genetics of parkinsonism. Parkinsonism Relat. Disord. 2007; 13 Suppl. 3:S233–S241. [PubMed: 18267242]

Chen, CA.; Okayama, H. High-efficient transfection using calcium phosphate-DNA precipitate formed in BES. In: Ausubel, Fea, editor. Currents Protocols in Molecular Biology. New York: John Wiley & Sons, Inc; 1997. p. 917-919.

Courtneidge SA. Activation of the pp60c-src kinase by middle T antigen binding or by dephosphorylation. EMBO J. 1985; 4:1471–1477. [PubMed: 2411538]

Covy JP, Giasson BI. Identification of compounds that inhibit the kinase activity of leucine-rich repeat kinase 2. Biochem. Biophys. Res. Commun. 2009; 378:473–477. [PubMed: 19027715]

De Bondt HL, Rosenblatt J, Jancarik J, Jones HD, Morgan DO, Kim SH. Crystal structure of cyclin-dependent kinase 2. Nature. 1993; 363:595–602. [PubMed: 8510751]

Deng H, Le W, Guo Y, Hunter CB, Xie W, Jankovic J. Genetic and clinical identification of Parkinson's disease patients with LRRK2 G2019S mutation. Ann. Neurol. 2005; 57:933–934. [PubMed: 15929036]

Di Fonzo A, Rohe CF, Ferreira J, et al. A frequent LRRK2 gene mutation associated with autosomal dominant Parkinson's disease. Lancet. 2005; 365:412–415. [PubMed: 15680456]

Dobson AW, Erikson KM, Aschner M. Manganese neurotoxicity. Ann. N. Y. Acad. Sci. 2004; 101(2): 115–128. [PubMed: 15105259]

Elberg G, Li J, Leibovitch A, Shechter Y. Non-receptor cytosolic protein tyrosine kinases from various rat tissues. Biochim. Biophys. Acta. 1995; 1269:299–306. [PubMed: 7495884]

Forman MS, Lee VM, Trojanowski JQ. Nosology of Parkinson's disease: looking for the way out of a quackmire. Neuron. 2005; 47:479–482. [PubMed: 16102530]

Giasson BI, Van Deerlin VM. Mutations in LRRK2 as a cause of Parkinson's disease. Neurosignals. 2008; 16:99–105. [PubMed: 18097165]

Gilks WP, Abou-Sleiman PM, Gandhi S, et al. A common LRRK2 mutation in idiopathic Parkinson's disease. Lancet. 2005; 365:415–416. [PubMed: 15680457]

Gloeckner CJ, Kinkl N, Schumacher A, Braun RJ, O'Neill E, Meitinger T, Kolch W, Prokisch H, Ueffing M. The Parkinson disease causing LRRK2 mutation I2020T is associated with increased kinase activity. Hum. Mol. Genet. 2006; 15:223–232. [PubMed: 16321986]

Gloeckner CJ, Schumacher A, Boldt K, Ueffing M. The Parkinson disease-associated protein kinase LRRK2 exhibits MAPKKK activity and phosphorylates MKK3/6 and MKK4/7, in vitro. J. Neurochem. 2009; 109:959–968. [PubMed: 19302196]

Greggio E, Cookson MR. Leucine-rich repeat kinase 2 mutations and Parkinson's disease: three questions. ASN Neuro. 2009:1.

Greggio E, Jain S, Kingsbury A, Bandopadhyay R, Lewis P, Kaganovich A, van der Brug MP, Beilina A, Blackinton J, Thomas KJ, Ahmad R, Miller DW, Kesavapany S, Singleton A, Lees A, Harvey RJ, Harvey K, Cookson MR. Kinase activity is required for the toxic effects of mutant LRRK2/dardarin. Neurobiol. Dis. 2006; 23:329–341. [PubMed: 16750377]

Greggio E, Zambrano I, Kaganovich A, et al. The Parkinson disease-associated leucine-rich repeat kinase 2 (LRRK2) is a dimer that undergoes intramolecular autophosphorylation. J. Biol. Chem. 2008; 283:16906–16914. [PubMed: 18397888]

Hanks SK, Quinn AM, Hunter T. The protein kinase family: conserved features and deduced phylogeny of the catalytic domains. Science. 1988; 241:42–52. [PubMed: 3291115]

Henchcliffe C, Beal MF. Mitochondrial biology and oxidative stress in Parkinson disease pathogenesis. Nat. Clin. Pract. Neurol. 2008; 4:600–609. [PubMed: 18978800]

Hernandez D, Paisan RC, Crawley A, Malkani R, Werner J, Gwinn-Hardy K, Dickson D, Wavrant DF, Hardy J, Singleton A. The dardarin G2019S mutation is a common cause of Parkinson's disease but not other neurodegenerative diseases. Neurosci. Lett. 2005; 389:137–139. [PubMed: 16102903]

Hoehn MM, Yahr MD. Parkinsonism: onset, progression and mortality. Neurology. 1967; 17:427–442. [PubMed: 6067254]

Huang CY, Yuan CJ, Luo S, Graves DJ. Mutational analyses of the metal ion and substrate binding sites of phosphorylase kinase gamma subunit. Biochemistry. 1994; 33:5877–5883. [PubMed: 8180216]

Hunter T, Cooper JA. Protein-tyrosine kinases. Annu. Rev. Biochem. 1985; 54:897–930. [PubMed: 2992362]

Jaleel M, Nichols RJ, Deak M, Campbell DG, Gillardon F, Knebel A, Alessi DR. LRRK2 phosphorylates moesin at threonine-558: characterization of how Parkinson's disease mutants affect kinase activity. Biochem. J. 2007; 405:307–317. [PubMed: 17447891]

Kachergus J, Mata IF, Hulihan M, et al. Identification of a novel LRRK2 mutation linked to autosomal dominant parkinsonism: evidence of a common founder across European populations. Am. J. Hum. Genet. 2005; 76:672–680. [PubMed: 15726496]

Kannan N, Neuwald AF. Did protein kinase regulatory mechanisms evolve through elaboration of a simple structural component? J. Mol. Biol. 2005; 351:956–972. [PubMed: 16051269]

Karlsson R, Zheng J, Xuong N, Taylor SS, Sowadski JM. Structure of the mammalian catalytic subunit of cAMP-dependent protein kinase and an inhibitor peptide displays an open conformation. Acta Crystallogr. D. Biol. Crystallogr. 1993; 49:381–388. [PubMed: 15299513]

Knowles JR. Enzyme-catalyzed phosphoryl transfer reactions. Annu. Rev. Biochem. 1980; 49:877–919. [PubMed: 6250450]

Koland JG, Cerione RA. Activation of the EGF receptor tyrosine kinase by divalent metal ions: comparison of holoreceptor and isolated kinase domain properties. Biochim. Biophys. Acta. 1990; 1052:489–498. [PubMed: 2354210]

Kornev AP, Haste NM, Taylor SS, Eyck LF. Surface comparison of active and inactive protein kinases identifies a conserved activation mechanism. Proc. Natl. Acad. Sci. U. S. A. 2006; 103:17783–17788. [PubMed: 17095602]

Lesage S, Durr A, Tazir M, Lohmann E, Leutenegger AL, Janin S, Pollak P, Brice A. LRRK2 G2019S as a cause of Parkinson's disease in North African Arabs. N. Engl. J. Med. 2006; 354:422–423. [PubMed: 16436781]

Lesage S, Ibanez P, Lohmann E, et al. G2019S LRRK2 mutation in French and North African families with Parkinson's disease. Ann. Neurol. 2005; 58:784–787. [PubMed: 16240353]

Levinson NM, Kuchment O, Shen K, Young MA, Koldobskiy M, Karplus M, Cole PA, Kuriyan J. A Src-like inactive conformation in the abl tyrosine kinase domain. PLoS Biol. 2006; 4:e144. [PubMed: 16640460]

Lovitt B, Vanderporten EC, Sheng Z, Zhu H, Drummond J, Liu Y. Differential effects of divalent manganese and magnesium on the kinase activity of leucine-rich repeat kinase-2 (LRRK2). Biochemistry. 2010; 49:3092–3100. [PubMed: 20205471]

Luzon-Toro B, Rubio de la TE, Delgado A, Perez-Tur J, Hilfiker S. Mechanistic insight into the dominant mode of the Parkinson's disease-associated G2019S LRRK2 mutation. Hum. Mol. Genet. 2007; 16:2031–2039. [PubMed: 17584768]

Manning G, Whyte DB, Martinez R, Hunter T, Sudarsanam S. The protein kinase complement of the human genome. Science. 2002; 298:1912–1934. [PubMed: 12471243]

Mata IF, Wedemeyer WJ, Farrer MJ, Taylor JP, Gallo KA. LRRK2 in Parkinson's disease: protein domains and functional insights. Trends Neurosci. 2006; 29:286–293. [PubMed: 16616379]

Nichols RJ, Dzamko N, Hutti JE, Cantley LC, Deak M, Moran J, Bamborough P, Reith AD, Alessi DR. Substrate specificity and inhibitors of LRRK2, a protein kinase mutated in Parkinson's disease. Biochem. J. 2009; 424:47–60. [PubMed: 19740074]

Nichols WC, Pankratz N, Hernandez D, et al. Genetic screening for a single common LRRK2 mutation in familial Parkinson's disease. Lancet. 2005; 365:410–412. [PubMed: 15680455]

Ozelius LJ, Senthil G, Saunders-Pullman R, et al. LRRK2 G2019S as a cause of Parkinson's disease in Ashkenazi Jews. N. Engl. J. Med. 2006; 354:424–425. [PubMed: 16436782]

Paisan-Ruiz C, Jain S, Evans EW, et al. Cloning of the gene containing mutations that cause PARK8-linked Parkinson's disease. Neuron. 2004; 44:595–600. [PubMed: 15541308]

Paisan-Ruiz C, Lang AE, Kawarai T, Sato C, Salehi-Rad S, Fisman GK, Al Khairallah T, George-Hyslop P, Singleton A, Rogaeva E. LRRK2 gene in Parkinson disease. Neurology. 2005; 65:696–700. [PubMed: 16157901]

Perl DP, Olanow CW. The neuropathology of manganese-induced Parkinsonism. J. Neuropathol. Exp. Neurol. 2007; 66:675–682. [PubMed: 17882011]

Puli S, Lai JCK, Edgley KL, Daniels CK, Bhushan A. Signaling pathways mediating manganese-induced toxicity in human glioblastoma cells (U87). Neurochem. Res. 2006; 31:1211–1218. [PubMed: 17043766]

Reichling LJ, Riddle SM. Leucine-rich repeat kinase 2 mutants I2020T and G2019S exhibit altered kinase inhibitor sensitivity. Biochem. Biophys. Res. Commun. 2009; 384:255–258. [PubMed: 19397894]

Ross OA, Farrer MJ. Pathophysiology, pleotrophy and paradigm shifts: genetic lessons from Parkinson's disease. Biochem. Soc. Trans. 2005; 33:586–590. [PubMed: 16042550]

Saylor P, Wang C, Hirai TJ, Adams JA. A second magnesium ion is critical for ATP binding in the kinase domain of the oncoprotein v-Fps. Biochemistry. 1998; 37:12624–12630. [PubMed: 9730835]

Simuni, T.; Hurtig, HI. Parkinson's disease: the clinical picture. In: Clark, CM.; Trojanoswki, JQ., editors. Neurodegenerative dementias. New York: McGraw-Hill; 2000. p. 193-203.

Smith WW, Pei Z, Jiang H, Dawson VL, Dawson TM, Ross CA. Kinase activity of mutant LRRK2 mediates neuronal toxicity. Nat. Neurosci. 2006; 9:1231–1233. [PubMed: 16980962]

Sun G, Budde RJ. Requirement for an additional divalent metal cation to activate protein tyrosine kinases. Biochemistry. 1997; 36:2139–2146. [PubMed: 9047313]

Taylor JP, Mata IF, Farrer MJ. LRRK2: a common pathway for parkinsonism, pathogenesis and prevention? Trends Mol. Med. 2006; 12:76–82. [PubMed: 16406842]

Taylor SS, Radzio-Andzelm E. Three protein kinase structures define a common motif. Structure. 1994; 2:345–355. [PubMed: 8081750]

Thomas B, Beal MF. Parkinson's disease. Hum. Mol. Genet. 2007; 16:R183–R194. Spec No. 2. [PubMed: 17911161]

Toru-Delbauffe D, Pierre M, Osty J, Chantoux F, Francon J. Properties of neurofilament protein kinase. Biochem. J. 1986; 235:283–289. [PubMed: 3461781]

Webber PJ, West AB. LRRKS in Parkinson's disease: function in cells and neurodegeneration. FEBS Lett. 2009; 276:6436–6444.

West AB, Moore DJ, Biskup S, Bugayenko A, Smith WW, Ross CA, Dawson VL, Dawson TM. Parkinson's disease-associated mutations in leucine-rich repeat kinase 2 augment kinase activity. Proc. Natl. Acad. Sci. U. S. A. 2005; 102:16842–16847. [PubMed: 16269541]

West AB, Moore DJ, Choi C, Andrabi SA, Li X, Dikeman D, Biskup S, Zhang Z, Lim KL, Dawson VL, Dawson TM. Parkinson's disease-associated mutations in LRRK2 link enhanced GTP-binding and kinase activities to neuronal toxicity. Hum. Mol. Genet. 2007; 16:223–232. [PubMed: 17200152]

Yuan CJ, Huang CY, Graves DJ. Phosphorylase kinase, a metal ion-dependent dual specificity kinase. J. Biol. Chem. 1993; 268:17683–17686. [PubMed: 8349652]

Zimprich A, Biskup S, Leitner P, et al. Mutations in LRRK2 cause autosomal-dominant parkinsonism with pleomorphic pathology. Neuron. 2004; 44:601–607. [PubMed: 15541309]

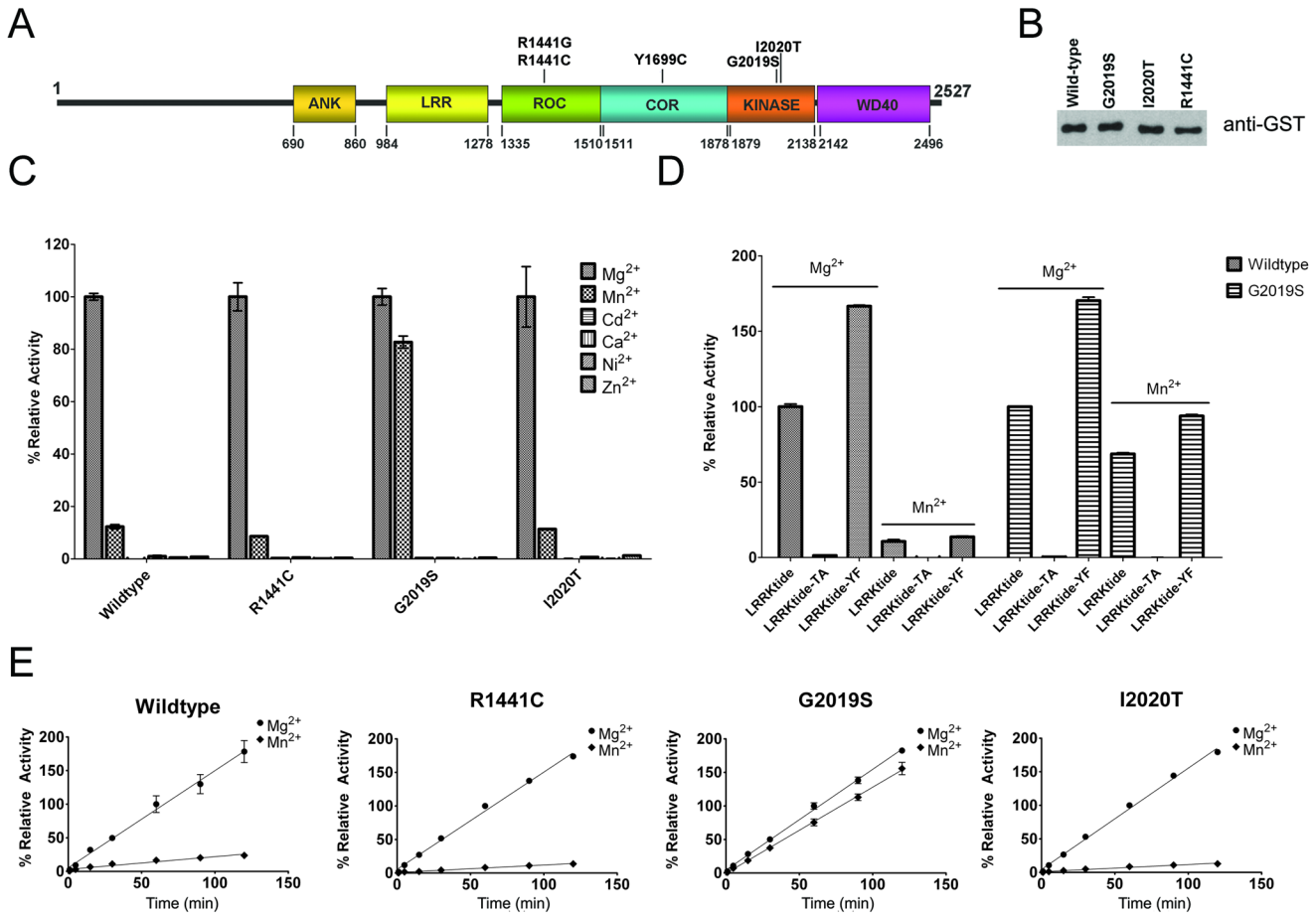

Figure 1. Characterization of recombinant LRRK2 kinase activity

(A) Schematic of LRRK2 showing the major domains [ankyrin-like (ANK), Leu-rich repeat (LRR), Ras-in-complex (ROC), C-terminal of RAS (COR)] and the position of the mutations that are considered definitely pathogenic. **(B)** Western blot with anti-GST antibody showing equal amounts of glutathione affinity-purified recombinant WT and mutant (G2019S, I2020T and R1441C) GST-LRRK2 full-length proteins. (**C**) Relative kinase activity of WT, R1441C, G2019S, and I2020T LRRK2 using 200 μM ATP, 400 μM LRRKtide and several individual divalent cations (Mg^{2+}, Mn^{2+}, Cd^{2+}, Ca^{2+}, Ni^{2+}, Zn^{2+}) at 5 mM. The data was standardized so that the phosphorylation reaction of LRRKtide with Mg^{2+} for each LRRK2 variant was normalized to 100%. (**D**) Comparative assessment of the ability of WT and G2019S LRRK2 to phosphorylate LRRKtide, LRRKtide-TA or LRRKtide-YF (300 μM each) in the presence of 200 μM ATP and either 5 mM Mg^{2+} or Mn^{2+}. (**E**) Assay demonstrating that the time-course of LRRK2 kinase activity was linear over 120 min using 200 μM ATP, 400 μM LRRKtide and either 5 mM Mg^{2+} or Mn^{2+}. For each LRRK2 variant, the activity was standardized as 100% for kinase reactions in 5 mM Mg^{2+} at 60 minutes. The error bars represent standard error of the mean.

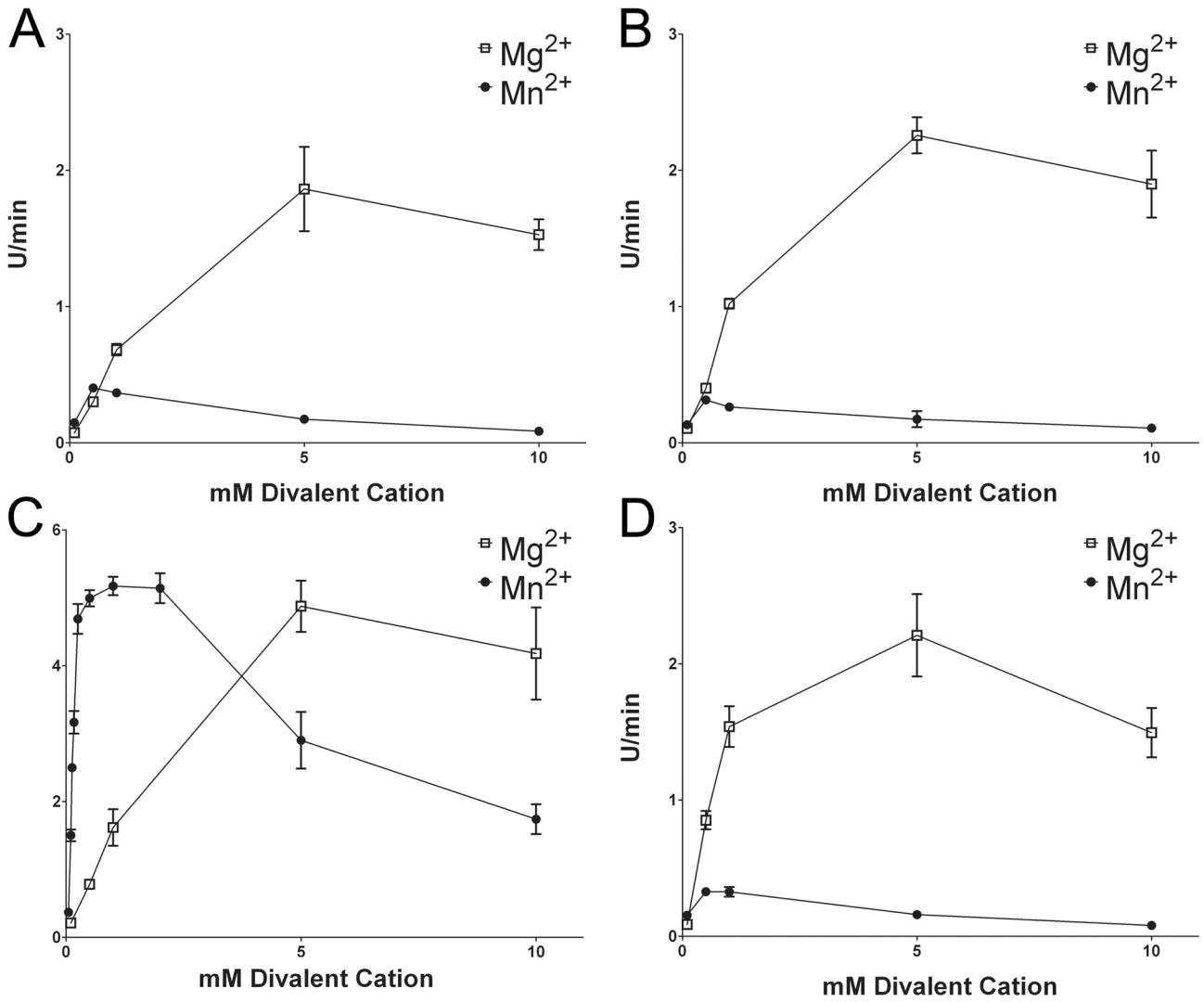

Figure 2. Concentration dependent affects of Mg^{2+} and Mn^{2+}on the kinase activity of WT, R1441C, G2019S, and I2020T LRRK2 on LRRKtide phosphorylation

Kinase reactions for (**A**) WT, (**B**) R1441C, (**C**) G2019S and (**D**) I2020T LRRK2 were conducted using 200μM ATP, 400μM LRRKtide and varying concentrations of Mg^{2+} or Mn^{2+} between 0.1 mM and 10 mM. The error bars represent standard error of the mean.

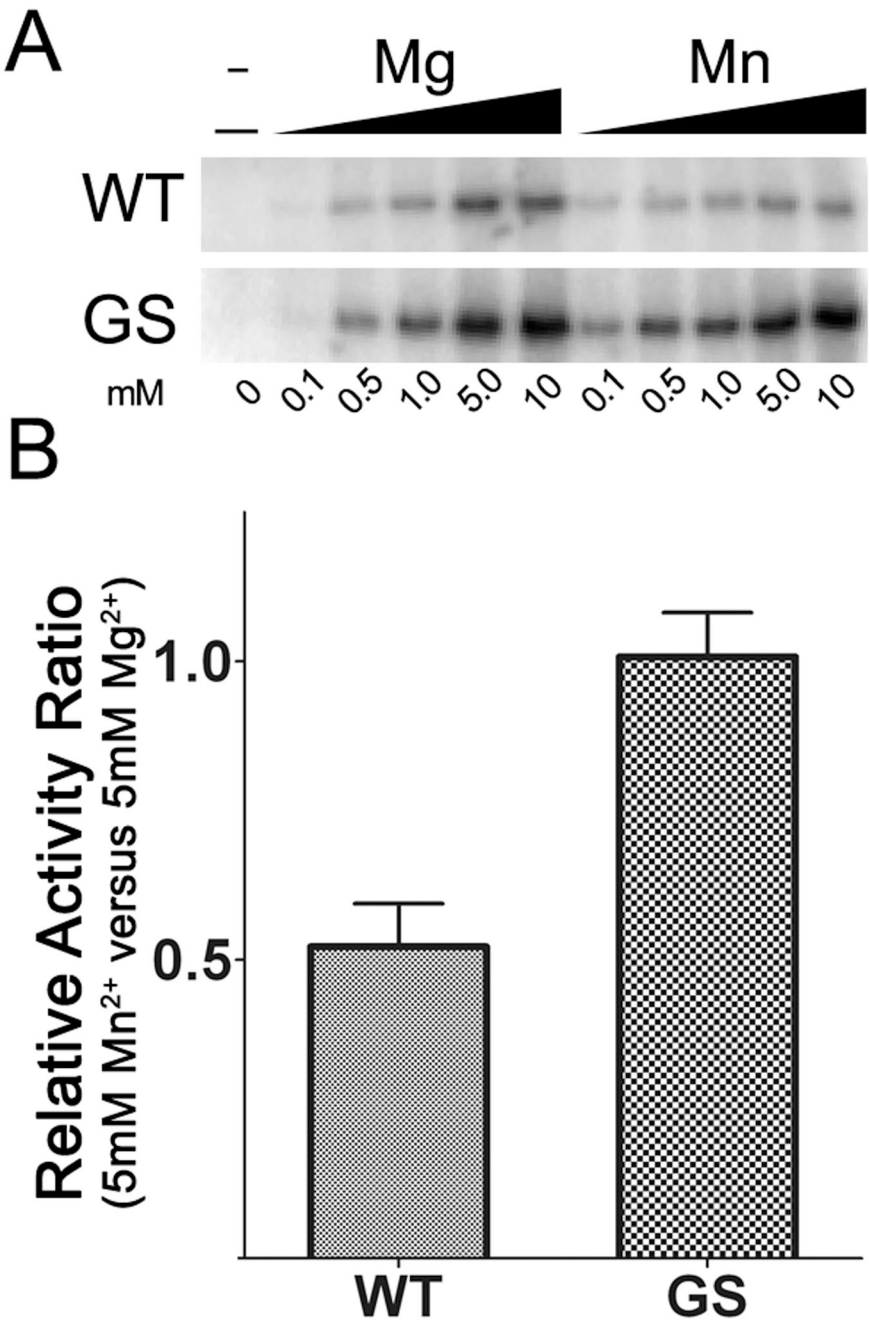

Figure 3. Concentration dependent affects of Mg^{2+} and Mn^{2}+ on the autophosphorylation activity of WT and G2019S LRRK2

(A) Kinase reactions for WT and G2019S were conducted using 100 uM ATP and with varying concentrations of divalent cation between 0.1 mM and 10 mM. Autoradiography shows the effects of increased concentration of Mg^{2+} or Mn^{2}+ autophosphorylation activity. (B) The relative activity of WT and G2019S LRRK2 when using either Mg^{2+} or Mn^{2+} as cofactor at 5 mM. The error bars represent standard error of the mean.

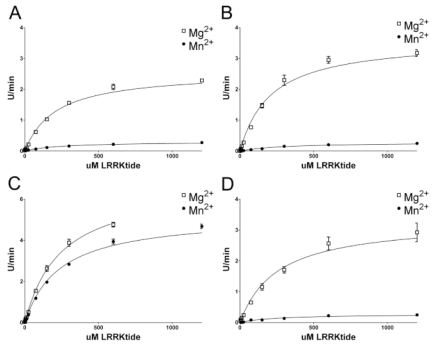

Figure 4. Kinetic characteristics of WT and LRRK2 mutations while varying the concentration of LRRKtide as a substrate

Assessment of the kinetic features of (**A**) WT, (**B**) R1441C, (**C**) G2019S and (**D**) I2020T recombinant LRRK2 with ATP at 200 μM with either 5 mM Mg^{2+} or 5 mM Mn^{2+}. The concentration of LRRKtide was varied as indicated on the x-axis. The error bars represent standard error of the mean.

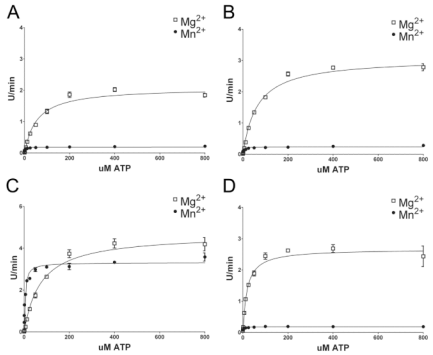

Figure 5. Kinetic characteristics of WT and LRRK2 mutations while varying the concentration of ATP as a substrate

Assessment of the kinetic features of (**A**) WT, (**B**) R1441C, (**C**) G2019S and (**D**) I2020T recombinant LRRK2 with LRRKtide at 400 μM with either 5 mM Mg^{2+} or 5 mM Mn^{2+}. The concentration of ATP was varied as indicated on the x-axis. The error bars represent standard error of the mean.

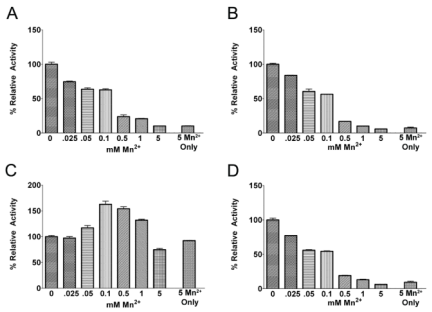

Figure 6. Analysis of effects of sub-stoichiometric concentrations of Mn^{2+} on WT and mutant LRRK2 kinase activity driven by Mg^{2+}

The activity of (A) WT, (B) R1441C, (C) G2019S and (D) I2020T recombinant LRRK2 was assessed in the presence of 200 μM ATP, 400 μM LRRKtide and 5 mM Mg^{2+} with concentrations of Mn^{2+} varying from 0–5 mM. As a reference, reactions with only 5 mM Mn^{2+} are also shown. For each LRRK2 variant, the activity was standardized as 100 % activity for kinase reactions with only 5 mM Mg^{2+}. The error bars represent standard error of the mean.

Table 1

Michaelis-Menton parameters of WT and LRRK2 mutations for LRRKtide

The relative apparent V_{max} (U/min) and K_m (μM) for LRRKtide were assessed with ATP at 200 μM and Mg^{2+} or Mn^{2+} at 5 mM. The errors represent standard deviations.

	Km						Vmax					
	Mg			Mn			Mg			Mn		
Wildtype	208.9	+/−	11.50	242.6	+/−	14.74	2.57	+/−	0.046	0.304	+/−	0.005
R1441C	208.6	+/−	17.30	300.5	+/−	30.55	3.63	+/−	0.102	0.286	+/−	0.009
G2019S	243.8	+/−	19.64	235.8	+/−	13.09	6.80	+/−	0.243	5.222	+/−	0.084
I2020T	251.7	+/−	37.80	255.5	+/−	35.91	3.31	+/−	0.146	0.282	+/−	0.012

Table 2

Michaelis-Menton parameters of wildtype and LRRK2 mutations for ATP

The relative apparent V_{max} (U/min) and K_m (μM) for ATP were assessed with LRRKtide at 400 μM and Mg^{2+} or Mn^{2+} at 5 mM. The errors represent standard deviations. LRRK2, leucine-rich repeat kinase-2.

	Km						Vmax					
	Mg			Mn			Mg			Mn		
Wildtype	54.53	+/−	4.73	1.40	+/−	0.173	2.08	+/−	0.044	0.189	+/−	0.003
R1441C	62.97	+/−	4.02	2.61	+/−	0.472	3.06	+/−	0.049	0.238	+/−	0.006
G2019S	74.08	+/−	7.73	3.93	+/−	0.436	4.68	+/−	0.126	3.315	+/−	0.057
I2020T	18.13	+/−	2.63	0.95	+/−	0.153	2.67	+/−	0.078	0.179	+/−	0.004